

Molecular electrometer and binding of cations to phospholipid bilayers

Andrea Catterall^a, Mykhailo Girych^b, Matti Javanainen^{cd}, Claire Loison^e, Josef Melcr^{fg}, Markus S. Miettinen^{hi}, Luca Monticelli^j, Jukka Määttä^k, Vasily S. Oganessian^a, O. H. Samuli Ollila^{*b}, Joonas Tynkkynen^c and Sergey Vilov^e

^aSchool of Chemistry, University of East Anglia, Norwich, NR4 7TJ, UK

^bDepartment of Neuroscience and Biomedical Engineering, Aalto University, Espoo, Finland. E-mail: samuli.ollila@aalto.fi

^cDepartment of Physics, Tampere University of Technology, Tampere, Finland

^dDepartment of Physics, University of Helsinki, Helsinki, Finland

^eUniv Lyon, Université Claude Bernard Lyon 1, CNRS, Institut Lumière Matière, F-69622, LYON, France

^fInstitute of Organic Chemistry and Biochemistry, Czech Academy of Sciences, Flemingovo nám. 2, 16610 Prague 6, Czech Republic

^gCharles University in Prague, Faculty of Mathematics and Physics, Ke Karlovu 3, 121 16 Prague 2, Czech Republic

^hFachbereich Physik, Freie Universität Berlin, Berlin, Germany

ⁱMax Planck Institute of Colloids and Interfaces, Department of Theory and Bio-Systems, Potsdam, Germany

^jInstitut de Biologie et Chimie des Protéines (IBCP), CNRS UMR 5086, Lyon, France

^kDepartment of Chemistry, Aalto University, Espoo, Finland

Despite the vast amount of experimental and theoretical studies on the binding affinity of cations – especially the biologically relevant Na^+ and Ca^{2+} – for phospholipid bilayers, there is no consensus in the literature. Here we show that by interpreting changes in the choline headgroup order parameters according to the ‘molecular electrometer’ concept [Seelig *et al.*, *Biochemistry*, 1987, **26**, 7535], one can directly compare the ion binding affinities between simulations and experiments. Our findings strongly support the view that in contrast to Ca^{2+} and other multivalent ions, Na^+ and other monovalent ions (except Li^+) do not specifically bind to phosphatidylcholine lipid bilayers at sub-molar concentrations. However, the Na^+ binding affinity was overestimated by several molecular dynamics simulation models, resulting in artificially positively charged bilayers and exaggerated structural effects in the lipid headgroups. While qualitatively correct headgroup order parameter response was observed with Ca^{2+} binding in all the tested models, no model had sufficient quantitative accuracy to interpret the Ca^{2+} :lipid stoichiometry or the induced atomistic resolution structural changes. All scientific contributions to this open collaboration work were made publicly, using nmrlipids.blogspot.fi as the main communication platform.

1 Introduction

Due to its high physiological importance – nerve cell signalling being the prime example – interaction of cations with phospholipid membranes has been widely studied via theory, simulations, and experiments. The relative ion binding affinities are generally agreed to follow the Hofmeister series,^{1–9} however, consensus on the quantitative affinities is currently lacking. Until 1990, the consensus (documented in two extensive reviews^{2,3}) was that while multivalent cations interact significantly with phospholipid bilayers, for monovalent cations (with the exception of Li^+) the interactions are weak. This conclusion has since been strengthened by further studies showing that bilayer properties remain unaltered upon the addition of sub-molar concentrations of monovalent

salt.^{4,10,11} Since 2000, however, another view has emerged, suggesting much stronger interactions between phospholipids and monovalent cations, and strong Na⁺ binding in particular.^{6–9,12–18}

The pre-2000 view has the experimental support that (in contrast to the significant effects caused by any multivalent cations) sub-molar concentrations of NaCl have a negligible effect on phospholipid infrared spectra,⁴ area per molecule,¹⁰ dipole potential,¹⁹ lateral diffusion,¹¹ and choline head group order parameters;²⁰ in addition, the water sorption isotherm of a NaCl–phospholipid system is highly similar to that of a pure NaCl solution – indicating that the ion–lipid interaction is very weak.⁴

The post-2000 ‘strong binding’ view rests on experimental and above all simulational findings. At sub-molar NaCl concentrations, the rotational and translational dynamics of membrane-embedded fluorescent probes decreased,^{7,9,12} and atomic force microscopy (AFM) experiments showed changes in bilayer hardness;^{14–18} in atomistic molecular dynamics (MD) simulations, phospholipid bilayers consistently bound Na⁺, although the binding strength depended on the model used.^{12,13,21–26}

Some observables have been interpreted in favour of both views. For example, as the effect of monovalent ions (except Li⁺) on the phase transition temperature is tiny (compared to the effect of multivalent ions), it was initially interpreted as an indication that only multivalent ions and Li⁺ specifically bind to phospholipid bilayers;² however, such a small effect in calorimetric measurements was later interpreted to indicate that also Na⁺ binds.^{8,12} Similarly, the lack of significant positive electrophoretic mobility of phosphatidylcholine (PC) vesicles in the presence of NaCl (again in contrast to multivalent ions and Li⁺) suggested weak binding of Na⁺;^{1,8,14,15,27} however, these data were also explained by a countering effect of the Cl[–] ions.^{22,28} Furthermore, to reduce the area per lipid in scattering experiments, molar concentrations of NaCl were required,¹⁰ indicating weak ion–lipid interaction; in MD simulations, however, already orders of magnitude lower concentrations resulted in Na⁺ binding and a clear reduction of area per lipid.^{12,23} Finally, lipid lateral diffusion was unaltered by NaCl in noninvasive NMR experiments;¹¹ however, as it was reduced upon Na⁺ binding in simulations, the reduced lateral diffusion of fluorescent probes^{7,9,12} has been interpreted to support the post-2000 ‘strong binding’ view.

In this paper, we set out to solve the apparent contradictions between the pre-2000 and post-2000 views. To this end, we employ the ‘molecular electrometer’ concept, according to which the changes in the C–H order parameters of the α and β carbons in the phospholipid head group (see Fig. 1) can be used to measure the ion affinity for a PC lipid bilayer.^{20,29–32} As the order parameters can be accurately measured in experiments and directly compared to simulations,³³ applying the molecular electrometer as a function of cation concentration allows the comparison of binding affinity between simulations and experiments. In addition to demonstrating the usefulness of this general concept, we show that the response of the α and β order parameters to penetrating cations is qualitatively correct in MD simulations, but that in several models the affinity of Na⁺ for PC bilayers is grossly overestimated. Moreover, we show that the accuracy of lipid–Ca²⁺ interactions in current models is not enough for atomistic resolution interpretation of NMR experiments.

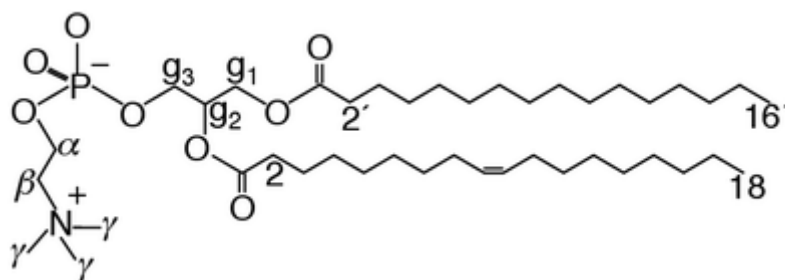


Fig. 1 Chemical structure of 1-palmitoyl-2-oleoylphosphatidylcholine (POPC), and the definition of γ , β , α , g_1 , g_2 and g_3 segments.

This work was done as an Open Collaboration at nmrlipids.blogspot.fi; all the related files³⁴ and almost all the simulation data (<https://zenodo.org/collection/user-nmrlipids>) are openly available.

2 Results and discussion

2.1 Background: molecular electrometer in experiments

The basis for the molecular electrometer is the experimental observation that binding of any charged objects (ions, peptides, anesthetics, amphiphiles) on a PC bilayer interface induced systematic changes in the choline α and β segment C–H order parameters.^{20,29–32,35–40} Being systematic, these changes could be employed for determining the binding affinities of the charged objects in question. Originally the molecular electrometer was devised for cations,^{20,29,30} but further experimental quantification with various positively and negatively charged molecules showed that the choline order parameters $S_{\alpha\text{CH}}$ and $S_{\beta\text{CH}}$ in general vary linearly with small amount of bound charge per lipid.^{30–32,35–40} Let now $S_{i\text{CH}}(0)$, where i refers to either α or β , denote the order parameter in the absence of bound charge; the empirically observed linear relation can then be written as⁴¹

$$\Delta S_{\text{CH}}^i = S_{\text{CH}}^i(X^\pm) - S_{\text{CH}}^i(0) = \frac{4m_i}{3\chi} X^\pm.$$

Here X^\pm is the amount of bound charge per lipid, m_i an empirical constant depending on the valency and position of bound charge, and the value of the quadrupole coupling constant $\chi \approx 167$ kHz.

With bound positive charge, the absolute value of the β segment order parameter increases and the α segment order parameter decreases (and vice versa for negative charge).^{20,29–32,35,40} However, as $S_{\beta\text{CH}}(0) < 0$ while $S_{\alpha\text{CH}}(0) > 0$,^{42–44} both $\Delta S_{\beta\text{CH}}$ and $\Delta S_{\alpha\text{CH}}$ in fact decrease with bound positive charge (and increase with bound negative charge). Consequently, values of m_i are negative for bound positive charges; for Ca^{2+} binding to POPC bilayer (in the presence of 100 mM NaCl), combination of atomic absorption spectra and ²H NMR experiments gave $m_\alpha = -20.5$ and $m_\beta = -10.0$.³⁰ This decrease can be rationalised by electrostatically induced tilting of the choline P–N dipole^{31,32,46} – also seen in simulations^{23,24,47,48} – and is in line with the order parameter increase related to the P–N vector tilting more parallel to the membrane plane seen with decreasing hydration levels.⁴⁵

Quantification of $\Delta S_{\alpha\text{CH}}$ and $\Delta S_{\beta\text{CH}}$ for a wide range of different cations (aqueous cations, cationic peptides, cationic anesthetics) has revealed that $\Delta S_{\beta\text{CH}}/\Delta S_{\alpha\text{CH}} \approx 0.5$.^{38,40} More specifically, the relation $\Delta S_{\beta\text{CH}} = 0.43\Delta S_{\alpha\text{CH}}$ was found to hold for DPPC bilayers at various CaCl_2 concentrations.²⁰

2.2 Molecular electrometer in MD simulations

The black curves in Fig. 2 show how the headgroup order parameters for DPPC and POPC bilayers change in ^2H NMR experiments as a function of salt solution concentration:20,30 Only minor changes are seen as a function of $[\text{NaCl}]$, but the effect of $[\text{CaCl}_2]$ is an order of magnitude larger. Thus, according to the molecular electrometer, the monovalent Na^+ ions have negligible affinity for PC lipid bilayers at concentrations up to 1 M, while binding of Ca^{2+} ions at the same concentration is significant.20,30

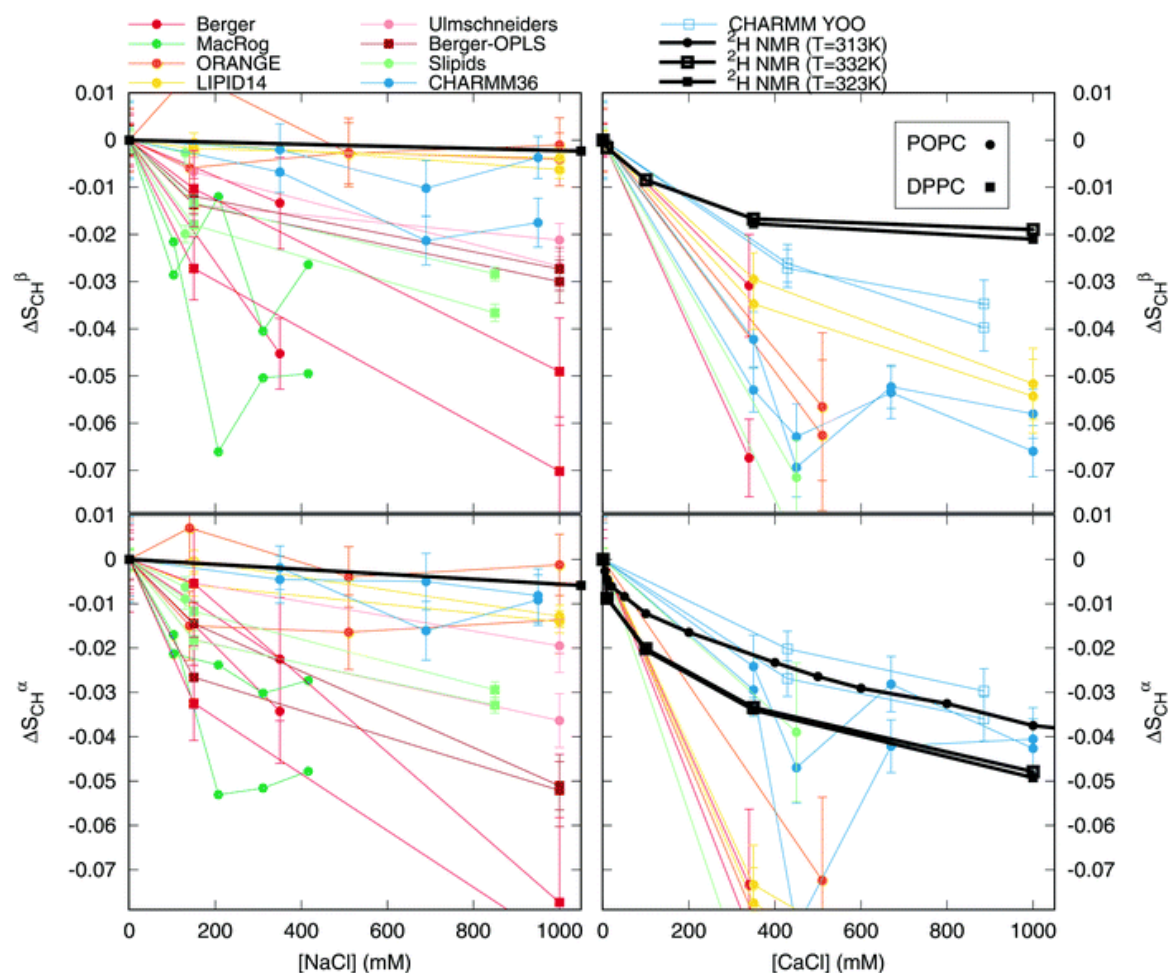


Fig. 2 Changes in the PC lipid headgroup β (top row) and α (bottom) segment order parameters in response to NaCl (left column) or CaCl_2 (right column) salt solution concentration increase. Comparison between simulations (Table 1) and experiments (DPPCs from ref. 20, POPC from ref. 30). The signs of the experimental values, from experiments without ions,^{42–44} can be assumed unchanged at these salt concentrations.^{30,33} We stress that none of the models reproduces the order parameters without salt within experimental error, indicating structural inaccuracies of varying severity in all of them.⁴⁵ Note that the relatively large drop in CHARMM36 at 450 mM CaCl_2 arose from more equilibrated binding due to a very long simulation time, see ESI.†

Fig. 2 also reports order parameter changes calculated from MD simulations of DPPC and POPC lipid bilayers as a function of NaCl or CaCl_2 initial concentrations in solution (for details of the simulated systems see Table 1 and ESI†). Note that although none of these MD models reproduces within experimental uncertainty the order parameters for a pure PC bilayer without ions (Fig. 2 in ref. 45), which indicates structural inaccuracies of varying severity in all models,⁴⁵ all the models qualitatively

reproduce the experimentally observed headgroup order parameter increase with dehydration.⁴⁵ Similarly here (Fig. 2) the presence of cations led to the decrease of S^{α}_{CH} and S^{β}_{CH} , in qualitative agreement with experiments. The changes were, however, overestimated by most models, which according to the molecular electrometer indicates overbinding of cations in most MD simulations.

Table 1 List of MD simulations. The salt concentrations calculated as $[\text{salt}] = N_c \times [\text{water}] / N_w$, where $[\text{water}] = 55.5 \text{ M}$; these correspond to the concentrations reported in the experiments by Akutsu *et al.*²⁰ The lipid force fields named as in our previous work⁴⁵

Force field for lipids	Lipid	Salt	[Salt] (mM)	N_c	N_w	N_s	$F(\text{D})$	$r_{\text{cut}}(\text{Å})$	$r_{\text{cut}}(\text{Å})$	Ref ⁴⁵
Beipen-DPPC ⁴² -FF _{lipid}	PDPG	NaCl	340	123	7302	44	298	110	50	21
Beipen-DPPC ⁴² -FF _{lipid}	PDPG	CaCl ₂	340	123	7177	44	298	103	50	21
Beipen-DPPC ⁴² -FF _{lipid}	PDPG	Na	0	72	2830	0	292	60	50	21
Beipen-DPPC ⁴² -FF _{lipid}	DPPG	NaCl	110	72	2830	8	312	120	120	21
Beipen-DPPC ⁴² -FF _{lipid}	DPPG	NaCl	1000	72	2718	21	312	120	120	21
Beipen-DPPC ⁴² -FF _{lipid}	DPPG	Na	0	72	2830	0	312	120	120	21
Beipen-DPPC ⁴² -FF _{lipid}	DPPG	NaCl	110	72	2830	8	312	120	120	21
Beipen-DPPC ⁴² -FF _{lipid}	DPPG	NaCl	1000	72	2718	21	312	120	120	21
Beipen-DPPC ⁴² -FF _{lipid}	PDPG	Na	0	72	2242	0	302	30	20	20
Beipen-DPPC ⁴² -FF _{lipid}	PDPG	NaCl	310	72	2032	13	302	60	60	20
Beipen-DPPC ⁴² -FF _{lipid}	PDPG	NaCl	680	72	2032	26	302	60	60	20
Beipen-DPPC ⁴² -FF _{lipid}	PDPG	NaCl	920	72	2148	37	302	60	60	20
Beipen-DPPC ⁴² -FF _{lipid}	PDPG	CaCl ₂	310	123	6400	31	302	100	200	21
Beipen-DPPC ⁴² -FF _{lipid}	PDPG	CaCl ₂	410	200	6400	31	302	100	200	21
Beipen-DPPC ⁴² -FF _{lipid}	PDPG	CaCl ₂	670	123	6400	67	302	120	200	21
Beipen-DPPC ⁴² -FF _{lipid}	PDPG	CaCl ₂	1000	123	6000	100	302	100	100	21
Beipen-DPPC ⁴² -FF _{lipid}	DPPG	Na	0	123	8000	0	312	170	170	—
Beipen-DPPC ⁴² -FF _{lipid}	DPPG	CaCl ₂	430	123	7160	60	312	200	200	—
Beipen-DPPC ⁴² -FF _{lipid}	DPPG	CaCl ₂	890	123	7250	120	312	200	200	—
Beipen-DPPC ⁴² -FF _{lipid}	PDPG	Na	0	123	6400	0	310	400	200	21
Beipen-DPPC ⁴² -FF _{lipid}	PDPG	Na	0	238	14400	0	310	40	40	21
Beipen-DPPC ⁴² -FF _{lipid}	PDPG	NaCl	100	238	14514	27	310	60	60	21
Beipen-DPPC ⁴² -FF _{lipid}	PDPG	NaCl	210	238	14500	54	310	60	60	21
Beipen-DPPC ⁴² -FF _{lipid}	PDPG	NaCl	310	238	14448	81	310	60	60	21
Beipen-DPPC ⁴² -FF _{lipid}	PDPG	NaCl	420	238	14382	108	310	60	60	21
Beipen-DPPC ⁴² -FF _{lipid}	PDPG	Na	0	72	2830	0	298	60	50	21
Beipen-DPPC ⁴² -FF _{lipid}	PDPG	NaCl	140	72	2830	7	298	120	120	21
Beipen-DPPC ⁴² -FF _{lipid}	PDPG	NaCl	1000	72	2730	26	298	120	120	21
Beipen-DPPC ⁴² -FF _{lipid}	PDPG	NaCl	1000	72	2730	26	298	120	120	21
Beipen-DPPC ⁴² -FF _{lipid}	PDPG	CaCl ₂	510	72	2832	28	298	120	120	21
Beipen-DPPC ⁴² -FF _{lipid}	PDPG	Na	0	123	1120	0	310	200	110	21
Beipen-DPPC ⁴² -FF _{lipid}	PDPG	NaCl	410	200	8000	21	310	200	200	21
Beipen-DPPC ⁴² -FF _{lipid}	PDPG	CaCl ₂	410	200	8000	21	310	200	200	21
Beipen-DPPC ⁴² -FF _{lipid}	PDPG	Na	0	123	3840	0	312	100	100	21
Beipen-DPPC ⁴² -FF _{lipid}	DPPG	NaCl	110	600	18000	48	312	100	40	21
Beipen-DPPC ⁴² -FF _{lipid}	DPPG	NaCl	1720	123	8728	27	312	202	202	21
Beipen-DPPC ⁴² -FF _{lipid}	DPPG	NaCl	1720	123	8421	144	312	202	202	21
Beipen-DPPC ⁴² -FF _{lipid}	DPPG	NaCl	2770	123	8314	163	312	202	202	21
Beipen-DPPC ⁴² -FF _{lipid}	PDPG	Na	0	123	5120	0	298	200	200	21
Beipen-DPPC ⁴² -FF _{lipid}	PDPG	NaCl	110	123	5120	12	298	200	200	21
Beipen-DPPC ⁴² -FF _{lipid}	PDPG	CaCl ₂	1000	123	5120	27	298	200	200	21
Beipen-DPPC ⁴² -FF _{lipid}	PDPG	CaCl ₂	1000	123	6400	100	298	200	200	21
Beipen-DPPC ⁴² -FF _{lipid}	PDPG	Na	0	123	7120	0	298	200	200	21
Beipen-DPPC ⁴² -FF _{lipid}	PDPG	NaCl	110	123	7120	12	298	200	200	21
Beipen-DPPC ⁴² -FF _{lipid}	PDPG	NaCl	1000	123	5120	77	298	200	200	21

^a Number of lipid molecules. ^b Number of water molecules. ^c Number of calcium. ^d Simulation temperature. ^e Total simulation time. ^f Force field for water. ^g Reference for simulation box.

While the molecular electrometer is well established in experiments (see Section 2.1 above), it is not a priori clear that it works in simulations. The overestimated order parameter decrease could, in principle, arise from an exaggerated response of the choline headgroups to the binding cations, instead of overbinding. Therefore, to evaluate the usability of the molecular electrometer in MD simulations, we analysed the relation between cation binding and choline order parameter decrease in simulations.

According to the molecular electrometer, the order parameter changes are linearly proportional to the amount of bound cations (eqn (1)). Fig. 3 shows this proportionality in MD simulations (see ES1† for the definition of bound ions); in keeping with the molecular electrometer, a roughly linear correlation between bound cation charge and order parameter change was found in all the eight models. Note that quantitative comparison of the proportionality constants (i.e. slopes in Fig. 3) between different models and experimental slopes ($m\alpha = -20.5$ and $m\beta = -10.0$ for Ca^{2+} binding in DPPC bilayer in the presence of 100 mM NaCl) is not straightforward since the simulation slopes depend on the definition used for bound ions (see ES1†).

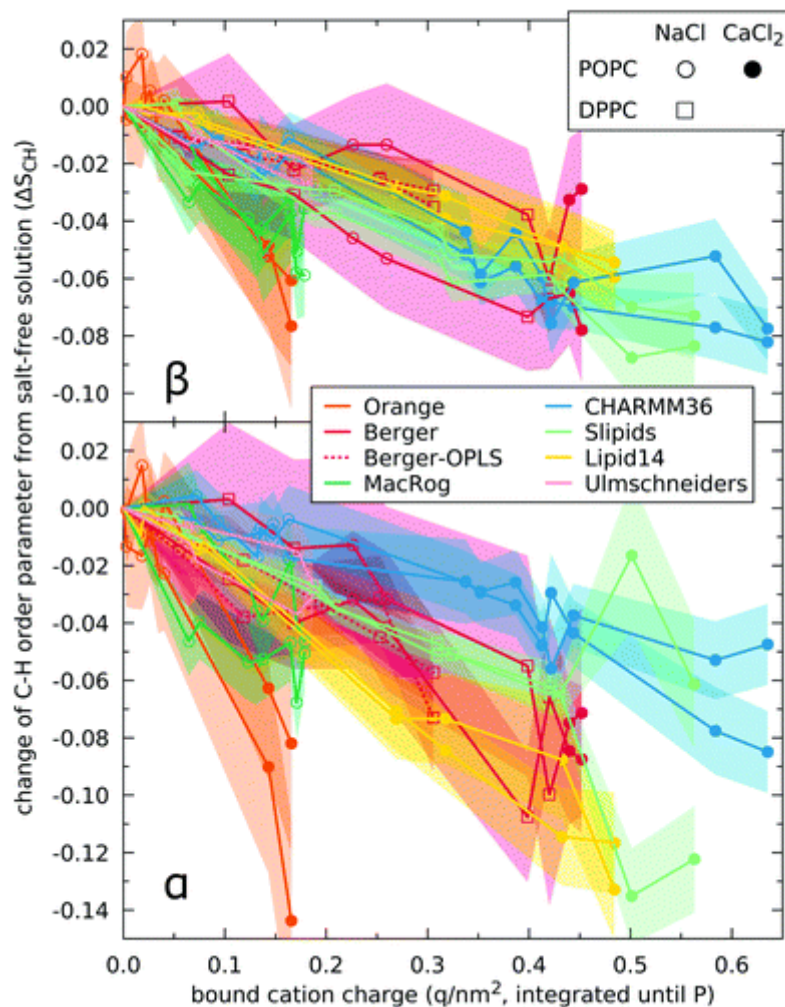


Fig. 3 Change of order parameters (from salt-free solution) of the β and α segments, $\Delta S_{\beta\text{CH}}$ and $\Delta S_{\alpha\text{CH}}$, as a function of bound cation charge. Eight MD simulation models compared; the two lines per model denote to the two hydrogens per carbon. The order parameters as well as the bound charge calculated separately for each leaflet; cations residing between the bilayer centre and the

density maximum of phosphorus considered bound; error bars (shaded) show standard error of mean over lipids.

We note that the quantitative comparison of order parameter changes in response to bound charge should be more straightforward for systems with charged amphiphiles fully associated in the bilayer, as the amount of bound charge is then explicitly known in both simulations and experiments. In such a comparison between experiments^{32,49} and previously published Berger-model-based simulations,⁵⁰ we could not rule out overestimation of order parameter response to bound cations (slopes $m\alpha$ and $m\beta$), see ESI.[†] This might, in principle, explain the overestimated order parameter response of the Berger model to CaCl_2 , but not to NaCl (see discussion in ESI[†]). Since simulation data with charged amphiphiles are not available for other models, an extended comparison with different models is left for further studies.

Fig. 3 shows that the decrease of order parameters clearly correlated with the amount of bound cations in simulations. This is also evident from Fig. 4, which shows the Na^+ density profiles of the MD models ordered according to the order parameter change (in Fig. 2) from the smallest (top) to the largest (bottom). The general trend in the figure is that the Na^+ density peaks are larger for models with larger changes in order parameters, in line with the observed correlation between cation binding and order parameter decrease in Fig. 3.

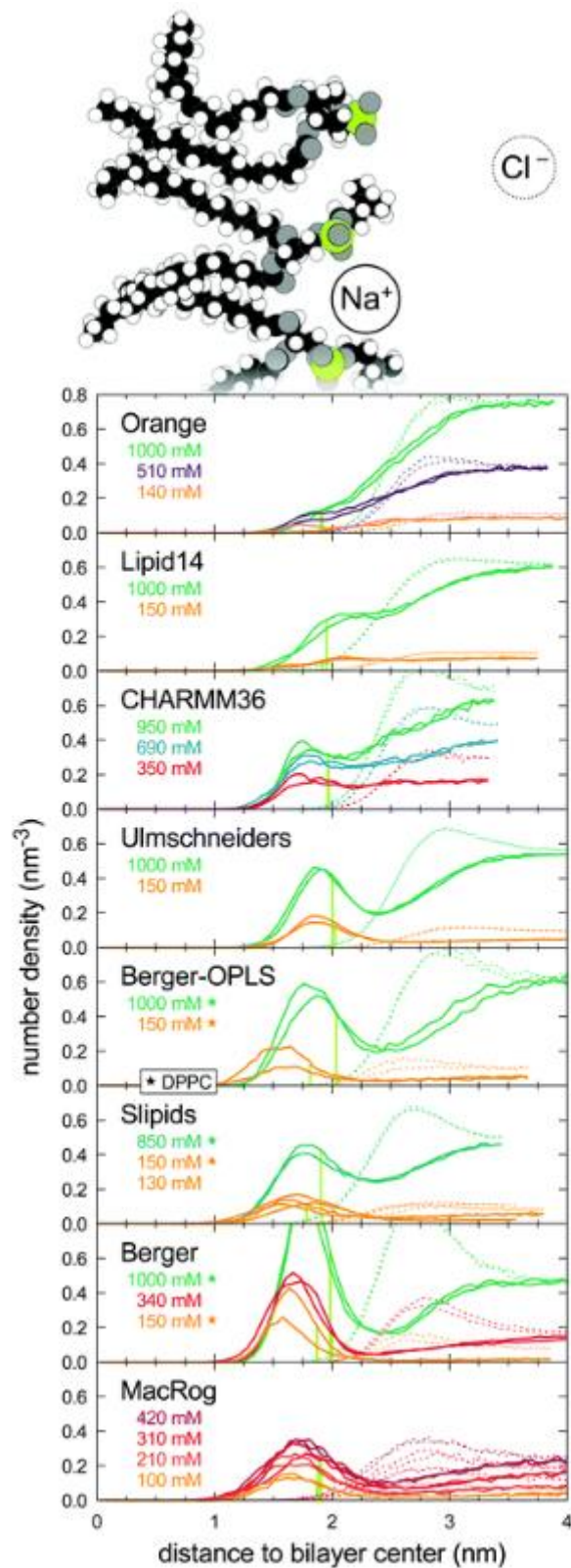


Fig. 4 Na⁺ (solid line) and Cl⁻ (dashed) distributions along the lipid bilayer normal from MD simulations at several NaCl concentrations. The eight MD models are ordered according to their strength of order parameter change in response to NaCl (Fig. 2) from the weakest (top panel) to the strongest (bottom). The light green vertical lines indicate the locations of the phosphorus maxima, used to define bound cations in Fig. 3.

Fig. 5 compares the relation between ΔS^{β}_{CH} and ΔS^{α}_{CH} in experiments20 and in MD models. Only Lipid14 gave $\Delta S^{\beta}_{CH}/\Delta S^{\alpha}_{CH}$ ratio in agreement with the experimental ratio; all other models underestimated the α segment order parameter decrease with bound cations with respect to the β segment decrease.

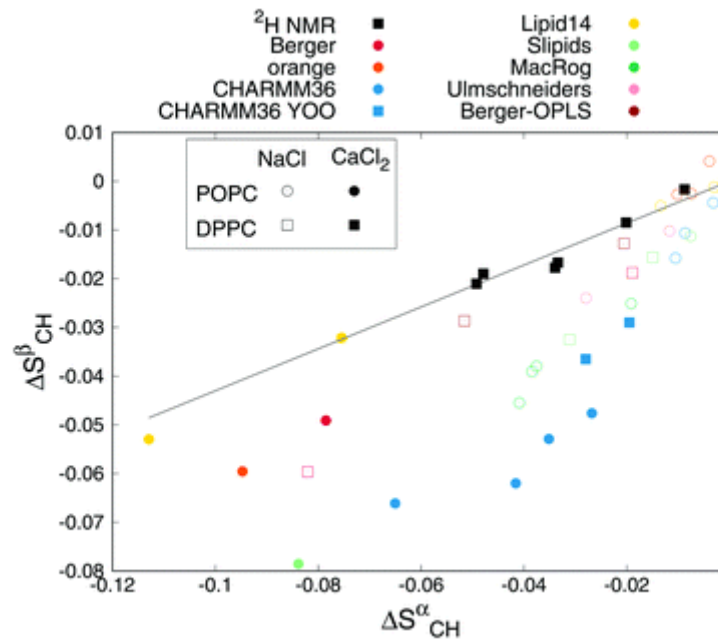


Fig. 5 Relation between ΔS^{β}_{CH} and ΔS^{α}_{CH} from experiments20 and different simulation models. Solid line is $\Delta S^{\beta}_{CH} = 0.43\Delta S^{\alpha}_{CH}$ determined for DPPC bilayer from 2H NMR experiment with various CaCl₂ concentrations.20

In conclusion, a clear correlation between bound cations and order parameter decrease was observed for all simulation models. Consequently, the molecular electrometer can be used to compare the cation binding affinity between experiments and simulations. However, we found that quantitatively the response of α and β segment order parameters to bound cations in simulations did not generally agree with the experiments; e.g., the $\Delta S^{\beta}_{CH}/\Delta S^{\alpha}_{CH}$ ratio agreed with experiments only in the Lipid14 model (Fig. 5). Thus, the observed overestimation of the order parameter changes with salt concentrations could, in principle, arise from overbinding of cations or from an oversensitive lipid headgroup response to the bound cations (see also discussion in ES1†). A careful analysis with current lipid models is performed in the next section

2.3 Cation binding in different simulation models

The order parameter changes (Fig. 2) and density distributions (Fig. 4) demonstrated significantly different Na⁺ binding affinities in different simulation models. The best agreement with experiments (lowest ΔS^{α}_{CH} and ΔS^{β}_{CH}) was observed for the three models (Orange, Lipid14, CHARMM36; see Fig. 2) that predicted the lowest Na⁺ densities near the bilayer (Fig. 4). All the other models clearly overestimated the choline order parameter responses to NaCl (Fig. 2) – and notably the strength of the overestimation was clearly linked to the strength of the Na⁺ binding affinity (compare Fig. 2 and 4), which leads us to conclude that Na⁺ binding affinity was overestimated in all these models.

As in the best three models the order parameter changes with NaCl were small (<0.02), the achieved statistical accuracy did not allow us to conclude which of the three had the most realistic Na⁺ binding affinity, especially at physiological NaCl concentrations (~ 150 mM) relevant for most

applications. The overestimated binding in the other models raises questions concerning the quality of predictions from these models when NaCl is present. Especially interactions between charged molecules and the bilayer might be significantly affected by the strong Na⁺ binding, which gives the otherwise neutral bilayer an effective positive charge.

Significant Ca²⁺ binding affinity for phosphatidylcholine bilayers at sub-molar concentrations is agreed on in the literature,^{2,3,20,30} however, several details remain under discussion. Simulations suggest that Ca²⁺ binds to lipid carbonyl oxygens with a coordination number of 4.2,¹³ while interpretation of NMR and scattering experiments suggest that one Ca²⁺ interacts mainly with the choline groups^{106–108} of two phospholipid molecules.³⁰ A simulation model correctly reproducing the order parameter changes would resolve the discussion by giving atomistic resolution interpretation for the experiments.

As a function of CaCl₂ concentration, all models but one (CHARMM36 with the recent heptahydrated Ca²⁺ by Yoo et al.⁷⁶) overestimated the order parameter decrease (Fig. 2), which according to the molecular electrometer indicates too strong Ca²⁺ binding. (We note that while this is the most likely scenario for the models that overestimated changes in both order parameters, for CaCl₂ it is possible also that the headgroup response is oversensitive to bound cations, see ESI.†) In CHARMM36 with the heptahydrated Ca²⁺ by Yoo et al.,⁷⁶ $\Delta S_{\beta CH}$ was overestimated but $\Delta S_{\alpha CH}$ underestimated (Fig. 2), in line with the $\Delta S_{\beta CH}/\Delta S_{\alpha CH}$ ratio in CHARMM36 being larger than in experiments (Fig. 5). As we do not know whether $\Delta S_{\beta CH}$ or $\Delta S_{\alpha CH}$ was more realistic, we cannot conclude whether Ca²⁺ binding was too strong or too weak in CHARMM36. This could be resolved by comparing against experimental data with a known amount of bound charge (e.g., amphiphilic cations^{32,49}), however, such simulation data are not currently available.

The density distributions with CaCl₂ showed significant Ca²⁺ binding in all models (Fig. 6), however, some differences occurred in details. The Berger model predicted deeper penetration (density maximum at ~1.8 nm) compared to other models (~2 nm); the latter value is probably more realistic as ¹H NMR and neutron scattering data indicate that Ca²⁺ interacts mainly with the choline group.^{2,106–108} In CHARMM36 (but not in Slipids) practically all Ca²⁺ ions present in the simulation bound the bilayer within 2 μ s (Fig. 6 and ESI†), which hints that the Ca²⁺ binding affinity of CHARMM36 is among the strongest of these models.

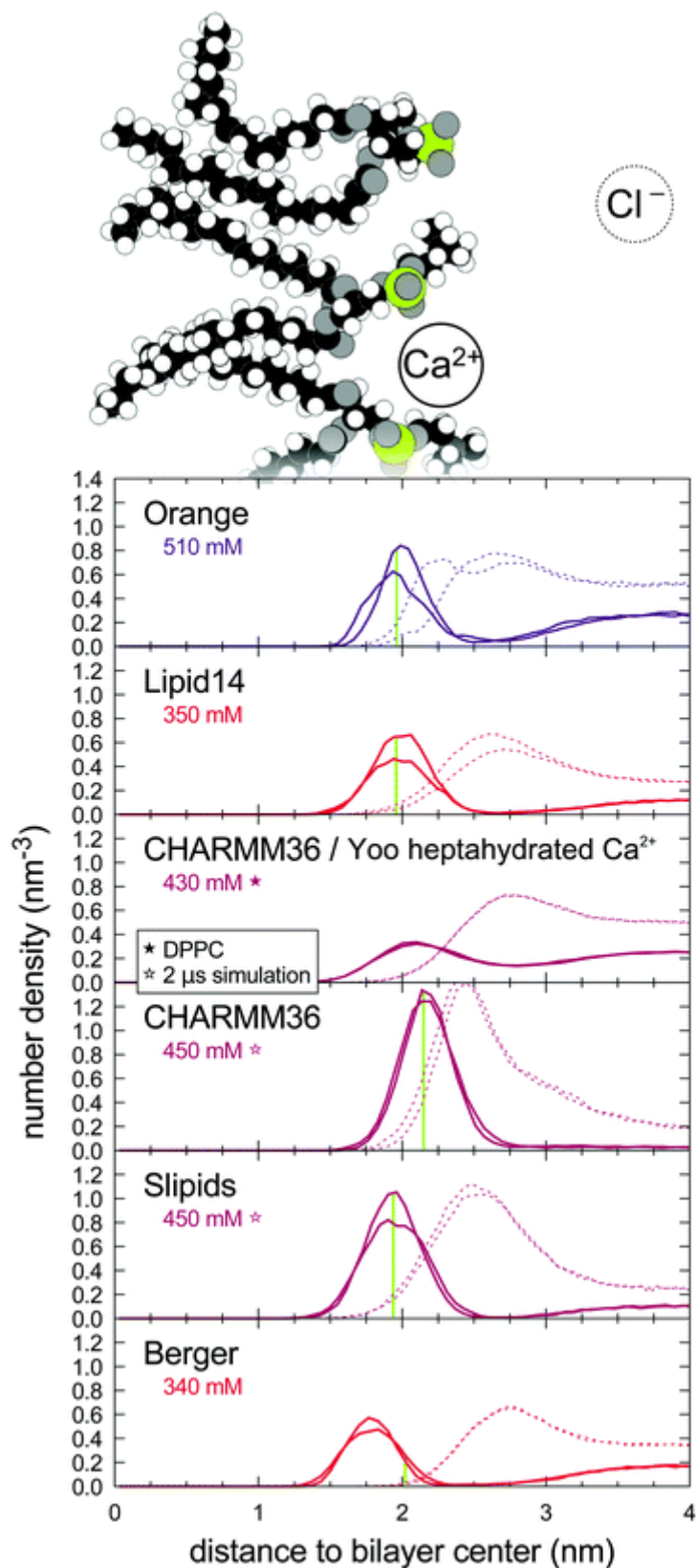


Fig. 6 Ca²⁺ (solid line) and Cl⁻ (dashed) distributions along the lipid bilayer normal from MD simulations. For clarity, only one CaCl₂ concentration per MD model is shown; see ESI† for a plot including all the available concentrations. The light green vertical lines indicate the locations of the phosphorus maxima, used to define bound cations in Fig. 3.

The origin of inaccuracies in lipid–ion interactions and binding affinities is far from clear. Potential candidates are, e.g., discrepancies in the ion models,^{109–111} incomplete treatment of electronic polarizability,¹¹² and inaccuracies in the lipid headgroup description.⁴⁵

Considering the ion models, Cordomi et al.²⁴ showed the Na⁺ binding affinity to decrease when ion radius is increased; however, in their DPPC bilayer simulations (with the OPLS-AA force field¹¹³) even the largest Na⁺ radii still resulted in significant binding. In our results, the Slipids force field gave essentially similar binding affinity with ion parameters from ref. 88, 93 and 94 (Fig. 4). Further, compensation of missing electronic polarizability by scaling the ion charge^{112,114} reduced Na⁺ binding in Berger, Berger-OPLS and Slipids, but not enough to reach agreement with experiments (ESI⁺). The charge-scaled Ca²⁺ model¹¹⁵ slightly reduced binding in CHARMM36, but did not have significant influence in Slipids (ESI⁺). The heptahydrated Ca²⁺ ions by Yoo et al.⁷⁶ significantly reduced Ca²⁺ binding in CHARMM36 (Fig. 6), however, the model must be further analysed to fully interpret the results.

The lipid models may also have a significant influence on ion binding behaviour. For example, the same ion model and non-bonded parameters are used in Orange and Berger-OPLS,⁶⁰ but while Na⁺ ion binding affinity appeared realistic in Orange, it was significantly overestimated in Berger-OPLS (Fig. 4). However, realistic Na⁺ binding does not automatically imply realistic Ca²⁺ binding (see Orange, Lipid14, and CHARMM36 in Fig. 2) or realistic choline order parameter response to bound charge (see Orange and CHARMM36 in Fig. 5). It should also be noted that the low binding affinity of Na⁺ in CHARMM36 is due to the additional repulsion (NBFIX68) added between the sodium ions and lipid oxygens (ESI⁺), and that in the Ca²⁺ model by Yoo et al.⁷⁶ the calcium is forced to be solvated solely by water. Altogether, our results indicate that probably both, lipid and ion force field parameters, need improvement to correctly predict the cation binding affinity, and the associated structural changes.

3 Conclusions

In accordance with the molecular electrometer,^{20,29–32} cation binding to lipid bilayers was accompanied with a decrease in the C–H order parameters of the PC head group α and β carbons in all the simulation models tested (Fig. 3) – despite of the known inaccuracies in the actual atomistic resolution structures.⁴⁵ Hence, the molecular electrometer allowed a direct comparison of Na⁺ binding affinity between simulations and noninvasive NMR experiments. The comparison revealed that most models overestimated Na⁺ binding; only Orange, Lipid14, and CHARMM36 predicted realistic binding affinities. None of the tested models had the accuracy required to interpret the Ca²⁺:lipid stoichiometry or the induced structural changes with atomistic resolution.

Taken together, our results corroborate the pre-2000 view that at sub-molar concentrations, in contrast to Ca²⁺ and other multivalent ions,^{1–4,10,11,19,20,27,30} Na⁺ and other monovalent ions (except Li⁺) do not specifically bind to phospholipid bilayers. Concerning the interpretation of existing experimental data, our work supports Cevc's view² that the observed small shift in phase transition temperature is not indicative of Na⁺ binding. Further, our findings are in line with the noninvasive NMR spectroscopy work of Filippov et al.¹¹ that proved the results of ref. 7, 9 and 12 to be explainable by direct interactions between Na⁺ ions and fluorescent probes. Finally, as spectroscopic methods are in general more sensitive to atomistic details in fluid-like environment than AFM, our work indirectly suggests that the ion binding reported from AFM experiments on fluid-like lipid bilayer systems^{14–18} might be confounded with other physical features of the system. Concerning contradictions in MD simulation results, we reinterpret the strong Na⁺ binding as an artefact of several simulation models, e.g., the Berger model used in ref. 12 and 13.

The artificial specific Na⁺ binding in MD simulations may lead to doubtful results, as it effectively results in a positively charged phosphatidylcholine lipid bilayer even at physiological NaCl concentrations. Such a charged bilayer will have distinctly different interactions with charged objects than what a (more realistic) model without specific Na⁺ binding would predict. Furthermore, the overestimation of binding affinity may extend from ions to other positively charged objects, say, membrane protein segments. This would affect lipid–protein interactions and could explain, for example, certain contradicting results on electrostatic interactions between charged protein segments and lipid bilayers.^{116,117} In conclusion, more careful studies and model development on lipid bilayer-charged object interactions are urgently called for to make molecular dynamics simulations directly usable in a physiologically relevant electrolytic environment.

This work was done as a fully open collaboration, using nmrlipids.blogspot.fi as the communication platform. All the scientific contributions were communicated publicly through this blog or the GitHub repository.³⁴ All the related content and data are available at ref. 34.

Acknowledgements

AC and VSO wish to thank the Research Computing Service at UEA for access to the High Performance Computing Cluster; VSO acknowledges the Engineering and Physical Sciences Research Council in the UK for financial support (EP/L001322/1). MG acknowledges financial support from Finnish Center of International Mobility (Fellowship TM-9363). J. Melcr acknowledges computational resources provided by the CESNET LM2015042 and the CERIT Scientific Cloud LM2015085 projects under the program “Projects of Large Research, Development, and Innovations Infrastructure”. MSM acknowledges financial support from the Volkswagen Foundation (86110). LM acknowledges funding from the Institut National de la Sante et de la Recherche Medicale (INSERM). OHSO acknowledges Tiago Ferreira for very useful discussions, the Emil Aaltonen foundation for financial support, Aalto Science-IT project and CSC-IT Center for Science for computational resources

References

1. M. Eisenberg, T. Gresalfi, T. Riccio and S. McLaughlin, *Biochemistry*, 1979, **18**, 5213–5223
2. G. Cevc, *Biochim. Biophys. Acta, Rev. Biomembr.*, 1990, **1031**, 311–382
3. J.-F. Tocanne and J. Teissié, *Biochim. Biophys. Acta, Rev. Biomembr.*, 1990, **1031**, 111–142
4. H. Binder and O. Zschörnig, *Chem. Phys. Lipids*, 2002, **115**, 39–61
5. J. J. Garcia-Celma, L. Hatahet, W. Kunz and K. Fendler, *Langmuir*, 2007, **23**, 10074–10080
6. E. Leontidis and A. Aroti, *J. Phys. Chem. B*, 2009, **113**, 1460–1467
7. R. Vacha, S. W. I. Siu, M. Petrov, R. A. Böckmann, J. Barucha-Kraszewska, P. Jurkiewicz, M. Hof, M. L. Berkowitz and P. Jungwirth, *J. Phys. Chem. A*, 2009, **113**, 7235–7243
8. B. Klasczyk, V. Knecht, R. Lipowsky and R. Dimova, *Langmuir*, 2010, **26**, 18951–18958
9. F. F. Harb and B. Tinland, *Langmuir*, 2013, **29**, 5540–5546
10. G. Pabst, A. Hodzic, J. Strancar, S. Danner, M. Rappolt and P. Laggner, *Biophys. J.*, 2007, **93**, 2688–2696
11. A. Filippov, G. Orädd and G. Lindblom, *Chem. Phys. Lipids*, 2009, **159**, 81–87
12. R. A. Böckmann, A. Hac, T. Heimburg and H. Grubmüller, *Biophys. J.*, 2003, **85**, 1647–1655
13. R. A. Böckmann and H. Grubmüller, *Angew. Chem., Int. Ed.*, 2004, **43**, 1021–1024
14. S. Garcia-Manyes, G. Oncins and F. Sanz, *Biophys. J.*, 2005, **89**, 1812–1826
15. S. Garcia-Manyes, G. Oncins and F. Sanz, *Electrochim. Acta*, 2006, **51**, 5029–5036
16. T. Fukuma, M. J. Higgins and S. P. Jarvis, *Phys. Rev. Lett.*, 2007, **98**, 106101
17. U. Ferber, G. Kaggwa and S. Jarvis, *Eur. Biophys. J.*, 2011, **40**, 329–338
18. L. Redondo-Morata, G. Oncins and F. Sanz, *Biophys. J.*, 2012, **102**, 66–74
19. R. J. Clarke and C. Lüpfer, *Biophys. J.*, 1999, **76**, 2614–2624

20. H. Akutsu and J. Seelig, *Biochemistry*, 1981, **20**, 7366–7373
21. J. N. Sachs, H. Nanda, H. I. Petrache and T. B. Woolf, *Biophys. J.*, 2004, **86**, 3772–3782
22. M. L. Berkowitz, D. L. Bostick and S. Pandit, *Chem. Rev.*, 2006, **106**, 1527–1539
23. A. Cordoní, O. Edholm and J. J. Perez, *J. Phys. Chem. B*, 2008, **112**, 1397–1408
24. A. Cordoní, O. Edholm and J. J. Perez, *J. Chem. Theory Comput.*, 2009, **5**, 2125–2134
25. C. Valley, J. Perlmutter, A. Braun and J. Sachs, *J. Membr. Biol.*, 2011, **244**, 35–42
26. M. L. Berkowitz and R. Vacha, *Acc. Chem. Res.*, 2012, **45**, 74–82
27. S. A. Tatulian, *Eur. J. Biochem.*, 1987, **170**, 413–420
28. V. Knecht and B. Klasczyk, *Biophys. J.*, 2013, **104**, 818–824
29. M. F. Brown and J. Seelig, *Nature*, 1977, **269**, 721–723
30. C. Altenbach and J. Seelig, *Biochemistry*, 1984, **23**, 3913–3920
31. J. Seelig, P. M. MacDonald and P. G. Scherer, *Biochemistry*, 1987, **26**, 7535–7541
32. P. G. Scherer and J. Seelig, *Biochemistry*, 1989, **28**, 7720–7728
33. O. H. S. Ollila and G. Pabst, *Biochim. Biophys. Acta*, 2016, **1858**, 2512–2528
34. A. Catte, M. Girysh, M. Javanainen, C. Loison, J. Melcr, M. S. Miettinen, L. Monticelli, J. Määttä, V. S. Oganessian, O. H. S. Ollila, J. Tynkkynen and S. Vilov, *NMRLipids/lipid_ionINTERACTION: Final submission to Physical Chemistry Chemical Physics*, 2016
35. C. Altenbach and J. Seelig, *Biochim. Biophys. Acta*, 1985, **818**, 410–415
36. P. M. Macdonald and J. Seelig, *Biochemistry*, 1987, **26**, 1231–1240
37. M. Roux and M. Bloom, *Biochemistry*, 1990, **29**, 7077–7089
38. G. Beschiaschvili and J. Seelig, *Biochim. Biophys. Acta, Biomembr.*, 1991, **1061**, 78–84
39. F. M. Marassi and P. M. Macdonald, *Biochemistry*, 1992, **31**, 10031–10036
40. J. R. Rydall and P. M. Macdonald, *Biochemistry*, 1992, **31**, 1092–1099
41. T. M. Ferreira, R. Sood, R. Bärenwald, G. Carlström, D. Topgaard, K. Saalwächter, P. K. J. Kinnunen and O. H. S. Ollila, *Langmuir*, 2016, **32**, 6524–6533
42. M. Hong, K. Schmidt-Rohr and A. Pines, *J. Am. Chem. Soc.*, 1995, **117**, 3310–3311
43. M. Hong, K. Schmidt-Rohr and D. Nanz, *Biophys. J.*, 1995, **69**, 1939–1950
44. J. D. Gross, D. E. Warschawski and R. G. Griffin, *J. Am. Chem. Soc.*, 1997, **119**, 796–802
45. A. Botan, F. Favela-Rosales, P. F. J. Fuchs, M. Javanainen, M. Kanduč, W. Kulig, A. Lamberg, C. Loison, A. Lyubartsev, M. S. Miettinen, L. Monticelli, J. Määttä, O. H. S. Ollila, M. Retegan, T. Róg, H. Santuz and J. Tynkkynen, *J. Phys. Chem. B*, 2015, **119**, 15075–15088
46. J. Seelig, *Cell Biol. Int. Rep.*, 1990, **14**, 353–360
47. A. A. Gurtovenko, M. Miettinen, M. Karttunen and I. Vattulainen, *J. Phys. Chem. B*, 2005, **109**, 21126–21134
48. W. Zhao, A. A. Gurtovenko, I. Vattulainen and M. Karttunen, *J. Phys. Chem. B*, 2012, **116**, 269–276
49. C. M. Franzin, P. M. Macdonald, A. Polozova and F. M. Winnik, *Biochim. Biophys. Acta, Biomembr.*, 1998, **1415**, 219–234
50. M. S. Miettinen, A. A. Gurtovenko, I. Vattulainen and M. Karttunen, *J. Phys. Chem. B*, 2009, **113**, 9226–9234
51. S. Ollila, M. T. Hyvönen and I. Vattulainen, *J. Phys. Chem. B*, 2007, **111**, 3139–3150
52. O. H. S. Ollila, T. Ferreira and D. Topgaard, *MD simulation trajectory and related files for POPC bilayer (Berger model delivered by Tieleman, Gromacs 4.5)*, 2014 DOI:
53. T. P. Straatsma and H. J. C. Berendsen, *J. Chem. Phys.*, 1988, **89**, 5876–5886
54. O. H. S. Ollila, *MD simulation trajectory and related files for POPC bilayer with 340 mM NaCl (Berger model delivered by Tieleman, ffgmx ions, Gromacs 4.5)*, 2015
55. O. H. S. Ollila, *MD simulation trajectory and related files for POPC bilayer with 340 mM CaCl₂ (Berger model delivered by Tieleman, ffgmx ions, Gromacs 4.5)*, 2015
56. S.-J. Marrink, O. Berger, P. Tieleman and F. Jähnig, *Biophys. J.*, 1998, **74**, 931–943
57. J. Määttä, *DPPC_Berger*, 2015

58. J. Määttä, *DPPC_Berger_NaCl*, 2015
59. J. Määttä, *DPPC_Berger_NaCl_1Mol*, 2015
60. D. P. Tieleman, J. L. MacCallum, W. L. Ash, C. Kandt, Z. Xu and L. Monticelli, *J. Phys.: Condens. Matter*, 2006, **18**, S1221
61. J. Määttä, *DPPC_Berger_OPLS06*, 2015
62. J. Åqvist, *J. Phys. Chem.*, 1990, **94**, 8021–8024
63. J. Määttä, *DPPC_Berger_OPLS06_NaCl*, 2015
64. J. Määttä, *DPPC_Berger_OPLS06_NaCl_1Mol*, 2016
65. J. B. Klauda, R. M. Venable, J. A. Freites, J. W. O'Connor, D. J. Tobias, C. Mondragon-Ramirez, I. Vorobyov, A. D. Mackerell Jr. and R. W. Pastor, *J. Phys. Chem. B*, 2010, **114**, 7830–7843
66. H. Santuz, *MD simulation trajectory and related files for POPC bilayer (CHARMM36, Gromacs 4.5)*, 2015
67. O. H. S. Ollila and M. Miettinen, *MD simulation trajectory and related files for POPC bilayer (CHARMM36, Gromacs 4.5)*, 2015
68. R. M. Venable, Y. Luo, K. Gawrisch, B. Roux and R. W. Pastor, *J. Phys. Chem. B*, 2013, **117**, 10183–10192
69. O. H. S. Ollila, *MD simulation trajectory and related files for POPC bilayer with 350 mM NaCl (CHARMM36, Gromacs 4.5)*, 2015
70. O. H. S. Ollila, *MD simulation trajectory and related files for POPC bilayer with 690 mM NaCl (CHARMM36, Gromacs 4.5)*, 2015
71. O. H. S. Ollila, *MD simulation trajectory and related files for POPC bilayer with 950 mM NaCl (CHARMM36, Gromacs 4.5)*, 2015
72. M. Girych and O. H. S. Ollila, *POPC_CHARMM36_CaCl2_035Mol*, 2015
73. M. Javanainen, *POPC@310K, 450 mM of CaCl_2. Charmm36 with default Charmm ions*, 2016
74. M. Girych and O. H. S. Ollila, *POPC_CHARMM36_CaCl2_067Mol*, 2015
75. M. Girych and O. H. S. Ollila, *POPC_CHARMM36_CaCl2_1Mol*, 2015
76. J. Yoo, J. Wilson and A. Aksimentiev, *Biopolymers*, 2016, **105**, 752–763
77. A. Maciejewski, M. Pasenkiewicz-Gierula, O. Cramariuc, I. Vattulainen and T. Rog, *J. Phys. Chem. B*, 2014, **118**, 4571–4581
78. M. Javanainen and W. Kulig, *POPC/Cholesterol@310K. 0, 10, 40, 50 and 60 mol-% cholesterol. Model by Maciejewski and Rog*, 2015, DOI: [10.5281/zenodo.13877](https://doi.org/10.5281/zenodo.13877).
79. M. Javanainen, *POPC@310K, varying water-to-lipid ratio, Model by Maciejewski and Rog*, 2014
80. M. Javanainen and J. Tynkkynen, *POPC@310K, varying amounts of NaCl. Model by Maciejewski and Rog*, 2015
81. O. H. S. Ollila, J. Määttä and L. Monticelli, *MD simulation trajectory for POPC bilayer (Orange, Gromacs 4.5.)*, 2015
82. O. H. S. Ollila, J. Määttä and L. Monticelli, *MD simulation trajectory for POPC bilayer with 140 mM NaCl (Orange, Gromacs 4.5.)*, 2015
83. O. H. S. Ollila, J. Määttä and L. Monticelli, *MD simulation trajectory for POPC bilayer with 510 mM NaCl (Orange, Gromacs 4.5.)*, 2015
84. S. Ollila, J. Määttä and L. Monticelli, *MD simulation trajectory for POPC bilayer with 1000 mM NaCl (Orange, Gromacs 4.5.)*, 2015
85. O. H. S. Ollila, J. Määttä and L. Monticelli, *MD simulation trajectory for POPC bilayer with 510 mM CaCl_2 (Orange, Gromacs 4.5.)*, 2015
86. J. P. M. Jämbeck and A. P. Lyubartsev, *J. Chem. Theory Comput.*, 2012, **8**, 2938–2948
87. M. Javanainen, *POPC@310K, Slipids force field.*, 2015
88. D. E. Smith and L. X. Dang, *J. Chem. Phys.*, 1994, **100**, 3757–3766
89. M. Javanainen, *POPC@310K, 130 mM of NaCl. Slipids with ions by Smith & Dang*, 2015
90. M. Javanainen, *POPC@310K, 450 mM of CaCl_2. Slipids with default Amber ions*, 2016

91. J. P. M. Jämbeck and A. P. Lyubartsev, *J. Phys. Chem. B*, 2012, **116**, 3164–3179
92. J. Määttä, *DPPC_Slipids*, 2014
93. D. Beglov and B. Roux, *J. Chem. Phys.*, 1994, **100**, 9050–9063
94. B. Roux, *Biophys. J.*, 1996, **71**, 3177–3185
95. J. Melcr, *Simulation files for DPPC lipid membrane with Slipids force field for Gromacs MD simulation engine*, 2016
96. C. J. Dickson, B. D. Madej, G. A. Skjevik, R. M. Betz, K. Teigen, I. R. Gould and R. C. Walker, *J. Chem. Theory Comput.*, 2014, **10**, 865–879
97. M. Girych and O. H. S. Ollila, *POPC_AMBER_LIPID14_Verlet*, 2015
98. M. Girych and O. H. S. Ollila, *POPC_AMBER_LIPID14_NaCl_015Mol*, 2015
99. M. Girych and O. H. S. Ollila, *POPC_AMBER_LIPID14_NaCl_1Mol*, 2015
100. M. Girych and O. H. S. Ollila, *POPC_AMBER_LIPID14_CaCl2_035Mol*, 2015
101. M. Girych and O. H. S. Ollila, *POPC_AMBER_LIPID14_CaCl2_1Mol*, 2015
102. J. P. Ulmschneider and M. B. Ulmschneider, *J. Chem. Theory Comput.*, 2009, **5**, 1803–1813
103. M. Girych and O. H. S. Ollila, *POPC_Ulmschneider_OPLS_Verlet_Group*, 2015
104. M. Girych and O. H. S. Ollila, *POPC_Ulmschneider_OPLS_NaCl_015Mol*, 2015
105. M. Girych and O. H. S. Ollila, *POPC_Ulmschneider_OPLS_NaCl_1Mol*, 2015
106. H. Hauser, M. C. Phillips, B. Levine and R. Williams, *Nature*, 1976, **261**, 390–394
107. H. Hauser, W. Guyer, B. Levine, P. Skrabal and R. Williams, *Biochim. Biophys. Acta, Biomembr.*, 1978, **508**, 450–463
108. L. Herbette, C. Napolitano and R. McDaniel, *Biophys. J.*, 1984, **46**, 677–685
109. B. Hess, C. Holm and N. van der Vegt, *J. Chem. Phys.*, 2006, **124**, 164509
110. A. A. Chen and R. V. Pappu, *J. Phys. Chem. B*, 2007, **111**, 11884–11887
111. M. M. Reif, M. Winger and C. Oostenbrink, *J. Chem. Theory Comput.*, 2013, **9**, 1247–1264
112. I. Leontyev and A. Stuchebrukhov, *Phys. Chem. Chem. Phys.*, 2011, **13**, 2613–2626
113. W. L. Jorgensen, D. S. Maxwell and J. Tirado-Rives, *J. Am. Chem. Soc.*, 1996, **118**, 11225–11236
114. M. Kohagen, P. E. Mason and P. Jungwirth, *J. Phys. Chem. B*, 2016, **120**, 1454–1460
115. M. Kohagen, P. E. Mason and P. Jungwirth, *J. Phys. Chem. B*, 2014, **118**, 7902–7909
116. A. Arkhipov, Y. Shan, R. Das, N. Endres, M. Eastwood, D. Wemmer, J. Kuriyan and D. Shaw, *Cell*, 2013, **152**, 557–569
117. K. Kaszuba, M. Grzybek, A. Orłowski, R. Danne, T. Róg, K. Simons, Ü. Coskun and I. Vattulainen, *Proc. Natl. Acad. Sci. U. S. A.*, 2015, **112**, 4334–4339